

Military Technical College
Kobry El-Kobba
Cairo, Egypt



12-th International Conference
on
Aerospace Sciences &
Aviation Technology

HIGH TEMPERATURE DEFORMATION BEHAVIOR OF Al-SiC_p METAL MATRIX COMPOSITES

A.A. Mazen * and M.M. Emara**

ABSTRACT

Aluminum-silicon carbide (Al-SiC_p) metal matrix composite (MMC) materials were fabricated using the powder metallurgy (PM) techniques of hot compaction followed by hot extrusion. Different reinforcement weight fractions were used, i.e. 0, 2.5, 5, and 10 wt% SiC_p.

Hot tensile deformation tests were used to characterize the ductility deformation and strength at different temperatures, i.e. $T = 0.3 T_m$, $0.4 T_m$, $0.5 T_m$, and $0.6 T_m$ (where T_m is the absolute melting point of the matrix material), and at different strain rates, i.e. $\dot{\epsilon} = 2 \times 10^{-3} \text{ s}^{-1}$, and $0.6 T_m \text{ } 100 \times 10^{-3} \text{ s}^{-1}$. Brief microscopic examination was used to support the analysis of results.

It was found that the stress-strain behavior is dominated by work-hardening at the lower temperature range. The work-hardening exponent (n) decreased as T increased and as reinforcement weight fraction increased but increased as $\dot{\epsilon}$ increased.

As reinforcement weight fraction increased, considerable strengthening was achieved compared to the unreinforced matrix. The reinforcement particles dominated the plastic flow and reduced the effect of high temperature in reducing the flow stress. However, as reinforcement weight fraction increased, the tensile strength σ_u , as well as the yielded strength, σ_y were negatively affected specially at high deformation temperatures and at high strain rates. σ_u was found to be more negatively affected than σ_y . σ_y and σ_u of the unreinforced material increased as $\dot{\epsilon}$ increased, for all tested temperatures. As reinforcement particles were introduced to the matrix, the two parameters increased with strain rate up to $\dot{\epsilon} = 50 \times 10^{-3} \text{ s}^{-1}$, then decreased as $\dot{\epsilon} = 100 \times 10^{-3} \text{ s}^{-1}$. Maximum reduction in σ_y was obtained at $T = 0.4 T_m$ at $\dot{\epsilon} = 100 \times 10^{-3} \text{ s}^{-1}$. Ductility expressed by the strain to failure, ϵ_f , decreased with the increase in $\dot{\epsilon}$, for all investigated materials. Minimum ϵ_f was obtained for Al-10 wt% SiC_p as $T = 0.4 T_m$ and $\dot{\epsilon} = 100 \times 10^{-3} \text{ s}^{-1}$ was applied.

KEYWORDS

Metal matrix composites-powder metallurgy-tensile deformation-ductility-strength.

* Associate Professor, El-Menia University, Email : mazasaad@yahoo.com

** Research Associate

1- INTRODUCTION

Development of high temperature resisting materials has always been a challenge to materials scientists. The search for such materials in the last few decades resulted in the development of several materials starting from monolithic single crystals for use in turbine blades, to superalloys used in aircraft turbine component and nuclear reactors [1, 2].

During the last two decades, the search for a metal matrix composite material (MMC) to serve as a high temperature material received considerable interest. Most of this research concentrated on aluminum-based MMC's. The obvious advantages of these materials being their light weight, high strength/ weight ratio, which is comparable to that of steels [3], high resistance to corrosion and oxidation, etc.. Al-based MMC's are being used or being considered as a potential material for manufacturing of car engine linings, connecting rods, piston heads, small gears, etc. [4].

Several methods have been developed for the manufacturing of MMC's, e.g. liquid phase processing [5, 6], semisolid processing [7], and powder metallurgy (PM) techniques [8]. PM processing proved to produce better quality MMC's, since better control on reinforcement distribution is possible which produces materials with superior mechanical properties [8].

Many problems can develop in materials serving under high temperature conditions. High temperature materials experience high mobility of dislocations which could lead to unfavorable conditions of loss of resistance to deformation and loss of strength. Several deformation mechanisms are operative at high temperatures. These include static recovery, static recrystallization and their dynamic counterparts [9]. Depending on the deformation conditions, one or more mechanisms may operate simultaneously.

The main objectives in studying high temperature deformation characteristics of Al-based MMC's are to determine their strength and ductility characteristics, and-more importantly to determine the proper processing parameters to produce a sound defect-free secondary product.

The goal of the present work is to present an experimental study of the high temperature deformation behavior of Al-SiC_p MMC manufactured by powder metallurgy (PM) techniques. Effects of high temperature and strain rates on the behavior of Al-SiC_p MMC having different reinforcement weight fractions are investigated. This is the first of a two-part research aiming at studying the mechanical characteristics of Al-SiC_p MMC, and the constitutive equation controlling their high temperature deformation behavior.

2. EXPERIMENTAL DETAILS :

2-1 Materials

Prewieghed amounts of silicon carbide (SiC_p) powder (average grain size, 50 μm) were added to prewieghed amounts of pure aluminum powder (average size, 63 μm), to produce mixtures of the following compositions:

Al- 2.5 wt% SiC_p, Al- 5wt% SiC_p, and Al- 10wt% SiC_p. Besides, pure (unreinforced) aluminum powder was used to produce reference material designated as Al-0wt% SiC_p.

The mixtures were hot pressed in a single acting hard dies made of heat resisting steel, at a temperature of 450°C (723k) which was maintained for 3 hrs at a compaction stress of 150 MPa.

The produced hot pressed billets were then hot extruded at an extrusion ratio of 5 : 1 for densification and closure of residual internal porosity. The extruded bars were used as raw stock, out of which, tensile test specimens, Fig.1, were machined.

2.2 Testing and Microscopic Examinations :

Tensile tests were conducted in an Instron universal testing machine equipped with data acquisition system (DAS). The machine is also equipped with a movable split-furnace whose accuracy was $\pm 5^\circ\text{C}$.

Testing was conducted at the following temperatures: RT (298 k), 100°C (373 k), 200°C (473 k), and 300°C (573 k).

This temperature range encompasses cold working up to hot working deformation temperature range, i.e. $0.3 T_m$ up to $0.6 T_m$. At each of these deformation temperatures, the following strain rates were used $2 \times 10^{-3} \text{ s}^{-1}$, and $100 \times 10^{-3} \text{ s}^{-1}$.

Optical microscopy was used to examine the microstructures of the specimens before and after deformation, while scanning electron microscopy (SEM) was used to examine the fracture surfaces of the tested specimens.

3. ANALYSIS AND DISCUSSION OF RESULTS :

3.1 Stress- Strain Behavior

Figure 2 through Fig. 5 show the stress-strain curves of the investigated MMC materials. These curves were calculated from the load-elongation curves obtained from the Instron universal testing machine.

The curves show a general form of metallic stress-strain behavior, i.e. elastic deformation, gradual yielding, plastic deformation, and fracture. The plastic deformation range is strongly affected by the reinforcement weight fraction, deformation temperature, and applied strain rate.

All curves exhibit post yielding initial hardening at low strains. As deformation continues, the effect of the above-mentioned variables becomes clear.

At lower temperature range ($0.3 \leq T/T_m \leq 0.5$), the plastic deformation range is dominated by work-hardening. Work-hardening of MMC's is known to be the result of piling-up of dislocations against barriers to their motion which leads to entanglement of these dislocations, causing increased resistance to further slip and deformation, i.e. strain hardening [10]. Barriers to dislocation motion in MMC's microstructure consist of submicron solute atoms or impurities in the matrix material, matrix grain boundaries, and the hard brittle reinforcement particles.

The work-hardening rate of the composite is usually higher than that of the unreinforced matrix at the early stages of deformation. As deformation proceeds, the stress induced at the particle/matrix interface leads to the relaxation of the Orowan loops [11].

At higher strains, for low reinforcement weight fractions, the particles will contribute to work hardening due to the creation of geometrically necessary dislocations [12]. These dislocations are necessary to allow compatible deformation in the composite without formation of voids around the hard particles.

The stress-strain data of the present work were fitted to the power law :

$$\sigma = k \varepsilon^n \dots\dots\dots (1)$$

where σ , ε , k , n , are the true plastic stress, true plastic strain, strength coefficient, and work-hardening exponent, respectively. Table 1 shows the derived n-values based on this equation.

Table 1 : Variation of Exponent "n" ⁽¹⁾ With Different Conditions:

| Material | $T_1 = 0.3T_m$ | | | $T_2 = 0.4 T_m$ | | | $T_3 = 0.5 T_m$ | | | $T_4 = 0.6 T_m$ | | |
|-----------|-----------------------------|-----------------------|-----------------------|-----------------------|-----------------------|-----------------------|-----------------------|-----------------------|-----------------------|-----------------------|-----------------------|-----------------------|
| | $\dot{\varepsilon}_1^{(2)}$ | $\dot{\varepsilon}_2$ | $\dot{\varepsilon}_3$ | $\dot{\varepsilon}_1$ | $\dot{\varepsilon}_2$ | $\dot{\varepsilon}_3$ | $\dot{\varepsilon}_1$ | $\dot{\varepsilon}_2$ | $\dot{\varepsilon}_3$ | $\dot{\varepsilon}_1$ | $\dot{\varepsilon}_2$ | $\dot{\varepsilon}_3$ |
| Al-0 wt% | 0.210 | 0.3 | 0.28 | 0.19 | 0.28 | 0.21 | 0.19 | 0.20 | 0.18 | 0.17 | 0.16 | 0.16 |
| Al-2.5wt% | 0.210 | 0.19 | 0.26 | 0.18 | 0.15 | 0.18 | 0.16 | 0.20 | 0.17 | 0.14 | 0.18 | 0.17 |
| Al-5 wt% | 0.17 | 0.23 | 0.27 | 0.16 | 0.28 | 0.24 | 0.15 | 0.17 | 0.15 | 0.03 | 0.06 | 0.10 |
| Al-10 wt% | 0.14 | 0.20 | 0.07 | 0.17 | 0.19 | 0.16 | 0.16 | 0.24 | 0.13 | 0.06 | 0.09 | 0.23 |

- (1) n = work hardening exponent,
- (2) $\dot{\varepsilon}_1 = 2 \times 10^{-3} \text{ s}^{-1}$, $\dot{\varepsilon}_2 = 50 \times 10^{-3} \text{ s}^{-1}$, $\dot{\varepsilon}_3 = 100 \times 10^{-3} \text{ s}^{-1}$

It is clear that the exponent n decreases as the deformation temperature increases, and at higher reinforcement weight fraction. It also increases as the strain rate increases. These factors involve softening and nucleation of voids, micro cracking of reinforcement particles due to higher deformation stresses, or presence of residual porosity and voids in-between clusters of particles at higher reinforcement weight fractions.

3-2 Effect of Reinforcement Weight Fraction :

Table 2 shows a comparison of the yield strength, σ_y , tensile strength, σ_u , and strain to fracture, ε_f for the different MMC's tested at $T = 0.3 T_m$ (room temperature), and $\dot{\varepsilon} = 2 \times 10^{-3} \text{ s}^{-1}$. Figs. 6a through 6d show variation of the same parameters, i.e. σ_y , σ_u , and ε_f , with deformation temperature as a function of the strain rate.

Table 2 : Comparison of σ_y , σ_u , and ε_f (At $T = 0.3 T_m$ and $\dot{\varepsilon} = 2 \times 10^{-3} \text{ s}^{-1}$)

| Material | σ_y , MPa | σ_u , MPa | ε_f % |
|----------|------------------|------------------|-------------------|
| Al- 0wt% | 77.10 | 130.20 | 24.60 |
| Al-25wt% | 102.80 | 146.60 | 18.80 |
| Al-5wt% | 46.15 | 137.50 | 18.50 |
| Al-10wt% | 89.50 | 117.90 | 11.50 |

It is clear that adding hard particles to the soft aluminum matrix caused considerable strengthening compared to the unreinforced aluminum (Al- 0wt% SiC_p). The flow stress at low strain rates ($\dot{\varepsilon} = 2 \times 10^{-3} \text{ s}^{-1}$) for both unreinforced and reinforced aluminum decreased monotonically as the deformation temperature increased, Fig.6. However, the reduction in flow stress of the unreinforced aluminum is greater than that of the reinforced aluminum. Thus, it may be concluded that over most of the

temperature range, at $\dot{\epsilon} = 2 \times 10^{-3} \text{ s}^{-1}$, the reinforcement particles dominated the plastic flow behavior, and compensated for the reduction caused by the temperature effect.

The improvement achieved in yield strength is greater than that achieved in the tensile strength. Also, as the reinforcement weight fraction increased, the improvement in both yielding and tensile strengths diminished following the same trend, Fig. 6. Compared to unreinforced aluminum properties at $\dot{\epsilon} = 2 \times 10^{-3} \text{ s}^{-1}$, $T = 0.3 T_m$, we find that yield strength improvement ranged from 33.3 % for Al-2.5 wt% SiC_p, to 16% for Al-10 wt% SiC_p, the tensile strength, on the other hand, improved by 12.59%. For Al-2.5 wt% SiC_p, and decreased by 9.44% for Al-10 wt% SiC_p.

The mechanisms controlling the strength of MMC's can provide a possible explanation for these observations. Two different competing mechanisms interact to determine the strength of a composite material. Positive mechanisms that lead to strength improvement include : dislocation-particle interaction (Orowan's mechanism), this mechanism has significant effects only if the reinforcement particles are very small (less than 1 micron) [13], dislocations pile-up against barriers to their motion which was explained above, and strengthening due to thermal processing and thermal mismatch between the soft metallic matrix and the hard ceramic particles. On the other hand, several factors play a negative role and reduce the strength or cause softening of the material. These include residual porosity which is a characteristic of PM materials, presence of clusters of particles which could: (i) incorporate voids within the cluster, (ii) hinder good bonding between the matrix and the reinforcement particles, and (iii) could promote stress triaxiality in the nearby area of the composite [14, 15]. Another factor that could negatively affect the strength of the composite is reinforcement particle cracking during processing or during deformation [16]. Fig.7a, shows a micrograph of Al-5 wt% SiC_p showing cracked reinforcement particles and residual porosity close to them. Fig.7.b shows an SEM fractograph showing cluster of particles and dimples of different sizes.

Thus, it may be concluded here that as reinforcement weight fraction increases, the tensile strength is negatively affected because it is plastic-strain dependent, while yielding strength improves as it is more of elastic deformation dependent then it is of microstructural features of the matrix and its strain path.

3.3 Temperature Dependence of Ductility and Strength

As mentioned above, yield strength, S_y , tensile strength, S_u , and Strain to fracture, ϵ_f , are all affected strongly by the increase in deformation temperature.

It can be seen from Figs 6 and 7 above that as the temperature increased from 0.3 T_m to 0.5 T_m , at a strain rate of $\dot{\epsilon} = 2 \times 10^{-3} \text{ s}^{-1}$, the yield and tensile strengths of Al-0 wt% SiC_p were reduce by 27% and 16%, respectively. For the same increase in temperature, the strain to fracture increased by 20%.

Table 3 : Changes in S_y , S_u , and ϵ_f (As a function of temperature change *)

| Material | 0.3 – 0.5 T _m | | | 0.5 T _m to 0.6 T _m | | |
|----------|--------------------------|---------------------|---------------------|--|-------------------|---------------------|
| | $\Delta \sigma\%$ | $\Delta \sigma_u\%$ | $\Delta \epsilon_f$ | $\Delta \sigma_y$ | $\Delta \sigma_u$ | $\Delta \epsilon_f$ |
| Al- 0wt% | -27.7 | -16.0 | +19.5 | -26.7 | -39.6 | +1.36 |

| | | | | | | |
|------------|-------|-------|--------|-------|-------|-------|
| Al- 2.5wt% | -46.2 | 951.0 | +23.9 | -13.6 | -27.9 | +1.28 |
| Al- 5 wt% | -20.0 | -33.0 | + 32.4 | -46.8 | -54.8 | -28.5 |
| Al-wt% | -13.4 | -25.5 | +13.4 | -37.3 | -42.0 | +50.0 |

* $\dot{\epsilon} = 2 \times 10^{-3} \text{ s}^{-1}$

As the temperature increased from 0.5 to 0.6 T_m , the yield strength was reduced by 26.7% while the tensile strength was reduced by about 40%. This proves that the tensile strength is more sensitive to temperature changes than the yield strength.

Table 3 indicates that as the temperature increased from 0.5 T_m to 0.6 T_m , the decrease in tensile strength was minimum for Al-2.5 wt% SiC_p , while the decrease under the same circumstances reached 54.8% for Al-5 wt% SiC_p , and 42% for Al-10 wt% SiC_p . This shows that materials with lower reinforcement weight fractions are more effective in temperature resistance than materials without reinforcement or materials with higher reinforcement weight fraction.

At a temperature of 0.6 T_m all investigated composites showed short initial hardening followed by constancy or even reduction in the flow curve, i.e. strain softening. Such behavior can be noticed for all compositions at all strain-rates. Thus, it could be considered as a rate independent, matrix-dependent behavior.

The main softening mechanisms operative in hot working ($T > 0.5 T_m$) are dynamic recovery (DRV), and dynamic recrystallization (DRX). In DRV, the [17] dislocations are rearranged into a substructure consisting of sub grains through the disintegration and reformation of subboundaries of constant spacing, thus, maintaining equiaxed subgrains [18]. In metals with high stacking fault energy (SFE), such as aluminum DRV appears to be quite effective. Mazen [19] found that in high temperature deformation of Al- Al_2O_3 MMC, both DRV and DRX seem to be operative. However, in most monolithic aluminum alloys, DRX was not reported because the level in most monolithic aluminum alloys because the level of DRV is so high that nucleation cannot occur during straining [20]. However, it was reported in case where constraints from hard particles enhance strain hardening and reduce DRV [21].

3.4 Strain Rate Dependence of Ductility and Strength :

As the applied initial strain rate increased from $\dot{\epsilon} = 2 \times 10^{-3} \text{ s}^{-1}$ to $100 \times 10^{-3} \text{ s}^{-1}$, the Al- 0wt % SiC_p composites showed an increase in σ_y and σ_u for all tested temperatures. The same trend was shown by σ_y for Al-2.5 wt% SiC_p . However, the σ_u of the latter composite was reduced by 7.8% as the strain rate increased from $50 \times 10^{-3} \text{ s}^{-1}$, to $100 \times 10^{-3} \text{ s}^{-1}$, at $T = 0.4 T_m$.

For Al-5 wt% SiC_p , at $T = 0.3 T_m$, the yield strength increased as a function of strain rate. However, at $T > 0.3 T_m$, the S_y decreased as the strain rate increased. The maximum decrease in S_y was shown at $T = 0.4 T_m$, $\dot{\epsilon} = 100 \times 10^{-3} \text{ s}^{-1}$. the tensile strength for Al-5 wt% SiC_p increased as $\dot{\epsilon}$ increased from 2×10^{-3} to $50 \times 10^{-3} \text{ s}^{-1}$, at all temperatures, then S_u decreased as $\dot{\epsilon}$ increased from $50 \times 10^{-3} \text{ s}^{-1}$ to $100 \times 10^{-3} \text{ s}^{-1}$, at all testing temperatures. The maximum reduction in S_u was obtained at $T = 0.4 T_m$, $\dot{\epsilon} = 100 \times 10^{-3} \text{ s}^{-1}$.

For Al-10 wt% SiC_p , a general trend of decrease in σ_y and σ_u was shown as $\dot{\epsilon}$ increased from $50 \times 10^{-3} \text{ s}^{-1}$ to $100 \times 10^{-3} \text{ s}^{-1}$. Maximum decrease of 9.1% in σ_y was shown for $T = 0.4 T_m$, $\dot{\epsilon} = 100 \times 10^{-3} \text{ s}^{-1}$.

The ductility expressed by strain to fracture, ε_f , showed a general decreasing trend as the strain rate increased for all investigated materials. The minimum ε_f was obtained for Al-10 wt% SiC_p at $\dot{\varepsilon} = 100 \times 10^{-3} \text{ s}^{-1}$, $T = 0.4 T_m$, figs. 8a through 8.d. showed the experimental results showed that the minimum yield and tensile strengths were always obtained for high strain rates, i.e. $\dot{\varepsilon} = 100 \times 10^{-3} \text{ s}^{-1}$ coupled with moderate deformation temperature, $T = 0.4 T_m$. High strain rates at such deformation temperatures are conducive for cavitations at matrix/particle interfaces [22]. Cavitations usually lead to premature termination of deformation. This may be a plausible explanation for the minimum ductility obtained at $T = 0.4 T_m$. On the other hand, high deformation temperature coupled with moderate strain rates are suitable conditions for restoration processes which lowers the flow stress and increase the ductility.

4- CONCLUSION :

An experimental study was conducted on Al-SiC_p PM metal matrix composites. The following conclusions can be derived based on this study :

- 1- the stress-strain behavior showed considerable strain hardening at room temperature, which was reduced as deformation temperature increased, and as higher reinforcement weight fractions were used. The hardening exponent increased as the strain rate increased, and decreased as deformation temperature increased, and as reinforcement weight fraction increased.
- 2- Over most of the temperature range, at low strain rates ($\dot{\varepsilon} = 2 \times 10^{-3} \text{ s}^{-1}$), the reinforcement particles dominated the plastic flow behavior and compensated for the reduction caused by the temperature effect.
- 3- The yield and tensile strengths increased as reinforcement weight fraction increased (up to 5 wt% SiC_p) and as the strain rate increased. The two variables decreased as the deformation temperature increased and as reinforcement weight fraction increased above 5 wt% SiC_p. However, the reduction in tensile strength was greater than that in the yield strength. This was attributed to the fact that tensile strength is more plastic strain dependent than the yield strength.
- 4- The yield and tensile strengths of unreinforced aluminum increased as the strain rate increased for all tested temperatures. The two parameters increased for reinforced aluminum up to a strain rate of $50 \times 10^{-3} \text{ s}^{-1}$.
- 5- Ductility increased as deformation temperature increased. It decreased with the increase of strain rate and reinforcement weight fraction. This was shown to be due to cavitations at matrix/particle interfaces.

REFERNCES :

- [1] Jacobus van Rensburg, "Automotive Materials", J. Adv. Mat. Processes, v. 164, No. 11. 2006, pp. 31-34.
- [2] I.A. Ibrahim, F.A. Mohamed, E.J. Lavernia, "Particulate Reinforced Metal Matrix Composites – A Review", J. Mater. Sci, V.26, 1991, P.1137.
- [3] A.L. Geiger and J.A. Walker, "Advances in Metal Matrix Composites", J. Metals, V. 43, 1991, p.8.

- [4] Val A.Kagan, "Advances in Automotive Materials", J. Adv. Mat. Processes, V. 161, no. 10, 2003, p. 37.
- [5] Graham Withers, "Dispersing Flyash Particles in an Aluminum Matrix", J. Adv. Mat. Processes, V. 164, no. 11, 2006, pp. 39-40.
- [6] S. Ray, "Synthesis of Cast Metal Matrix Composites, A Review", J. Mater. Sci., V. 28, 1993, pp 5397-5413.
- [7] E.M. Klier, A. Mortensen, J.A. Cornie, and M.C.Fleming, "Fabrication of Cast Particle-Reinforced Metals via Pressure Infiltration", J. Mater. Sci., V. 26, 1991, p. 2519.
- [8] Y. B. Lui, S.C. Lim, L. Lu, M.O. Lai, "Reinforcement Development in the Fabrication of Metal Matrix Composites Using Powder Metallurgy Techniques", J. Mater. Sci., V. 29, 1994, p. 1999.
- [9] A.Y. Ahmed, "Mechanical Behavior of Al-Al₂O₃ MMC Manufactured by PM Techniques", M.Sc. Thesis, The American University in Cairo, July 1997, p. 46.
- [10] A. Cottrell, Introduction to Metallurgy, 2nd Ed., Edward Arnold 1980, p. 386.
- [11] M.F. Ashby, in " Strengthening Methods in Crystals", A. Kelly, R.B. Nicholson, eds., El-Sevier, Amsterdam, 1971, p. 184.
- [12] W.S. Miller and F.J. Humphreys, "Strengthening Methods in Particulate Metal Matrix Composites", Scripta Metallurgica et Materialia, V25,1991, pp. 33-38.
- [13] M. Taya, and T. Mori, "Dislocation Punching from Ceramic particle interface", Trans. ASME, V 116, 1994, p. 408.
- [14] M. Taya, K.E. Luley, D.J. Liyd, "Strengthening of Particulate Metal Matrix Composites by Quenching", Acta Metal. Mater., V. 39, 1991, pp. 73-87.
- [15] S.I. Hong and G. T. Gray III, "Quenching and Thermal Cycling Effects in a 1060 Al-matrix-10 vol.% Al₂O₃ Particulate Composite" Mat. Sci. Eng. A, V. 171, 1993, PP. 181-189.
- [16] A.A. Mazen and M.M. Emara, "Effect of Particle Cracking on the Strength and Ductility of Al-SiC_p PM MMC", J. Mat. Eng. Perf., V. 13 (1), 2004, PP. 39-46.
- [17] H.J. McQueen, E. Evangelista, N. Jin, and M. E. Kassner, "Energy Dissipation Efficiency in Aluminum Dependent on Monotonic Flow Curves and Dynamic Recovery", Met. Mater. Trans. A, V. 26 A, 1995, pp. 1757 -1766.
- [18] P. Olla and P.F. Viridis, "High Temperature Deformation of a Commercial Aluminum Alloy", Met. Trans. A, V. 18A, 1987, pp. 293-302.
- [19] A.A. Mazen, "Effect of Deformation Temperature on the Mechanical Behavior and Deformation Mechanisms of Al-Al₂O₃ MMC", J. Mat. Eng. Perf., V.8 (4), 1999, pp. 487-495.
- [20] H.J. McQueen, "Hot Deformation of Aluminum Alloys", T. G. Langdon and H.D. Merchant, eds., TMS-AIME, Warrendale PA, 1991, pp. 31-54.
- [21] H.J. McQueen and M.E. Kassner, "Superplasticity in Aerospace II", T.R. McNelly, ed., TMS-AIMS, Warrandale, PA, 1990, pp. 189-206.
- [22] E. Evangelista and Spigarellu, " Constitutive Equations for Greep and PLAsticity in Aluminum Alloys Produced by PM and Aluminum-Based MMC", Met. Mater. Trans. A, Vol. 33A, 2002, pp. 372-381.

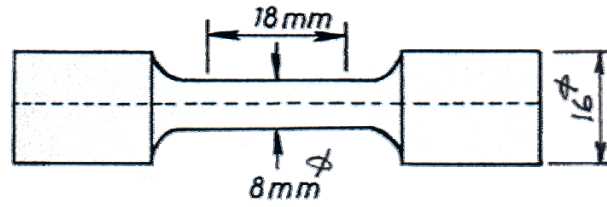


Fig. 1 Tensile Test Specimen

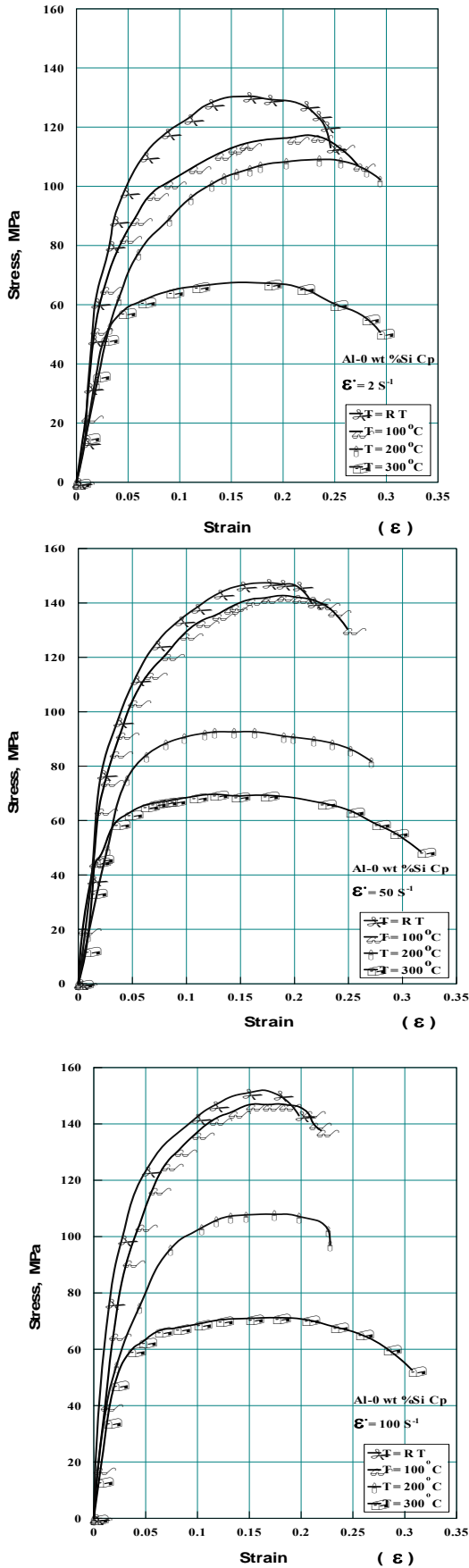


Fig. 2 Stress-Strain Curves for Al-0 wt% Si Cp at different temperature and strain rate

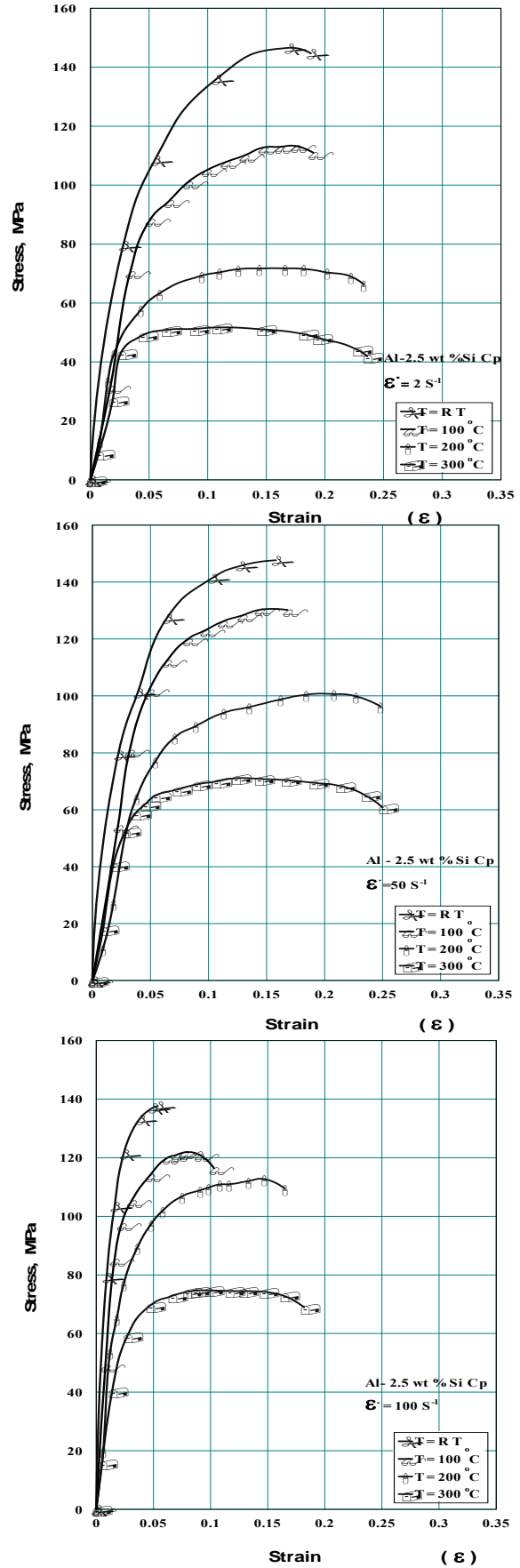


Fig. 3 Stress-Strain Curves for Al-2.5 wt% Si Cp at different temperature and strain rate

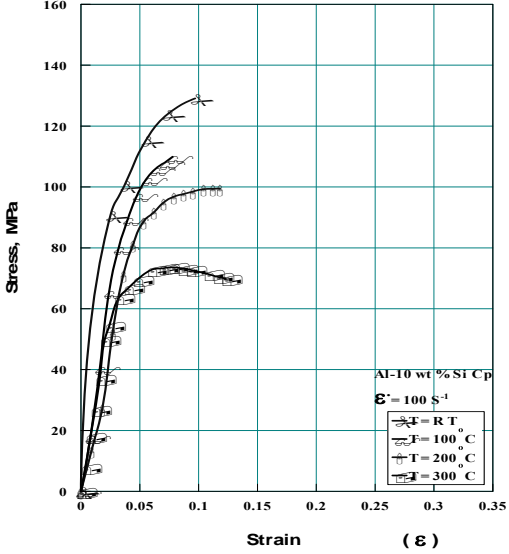
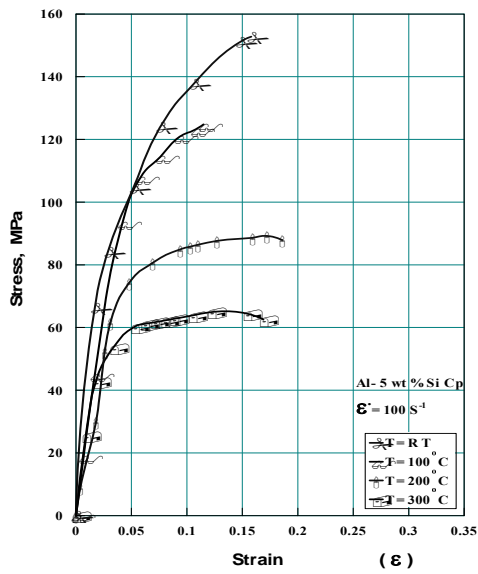
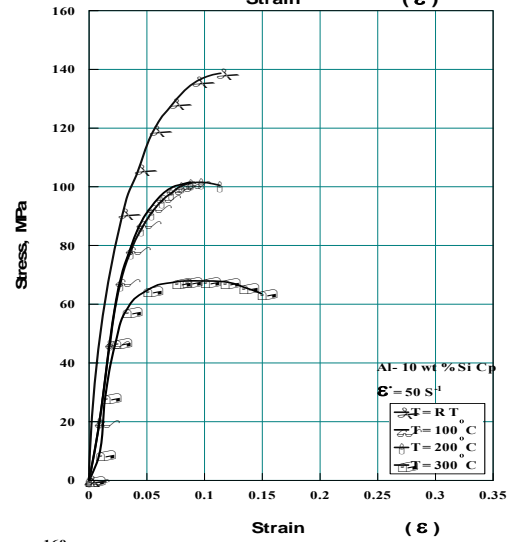
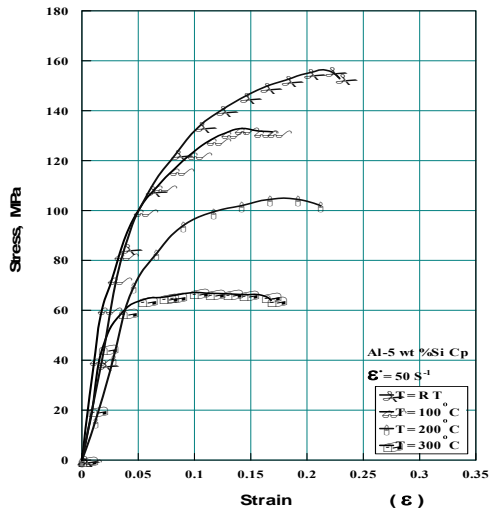
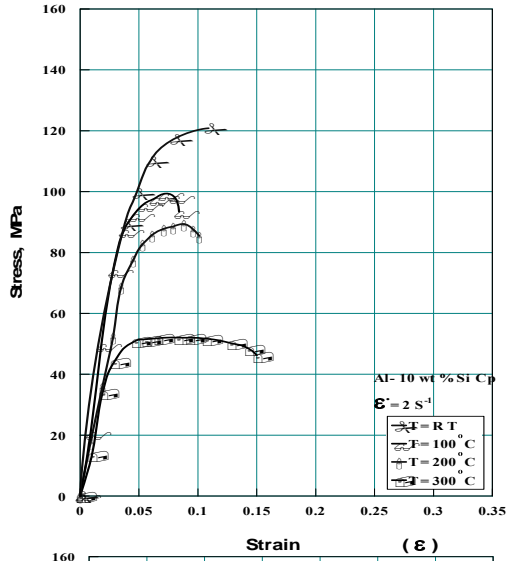
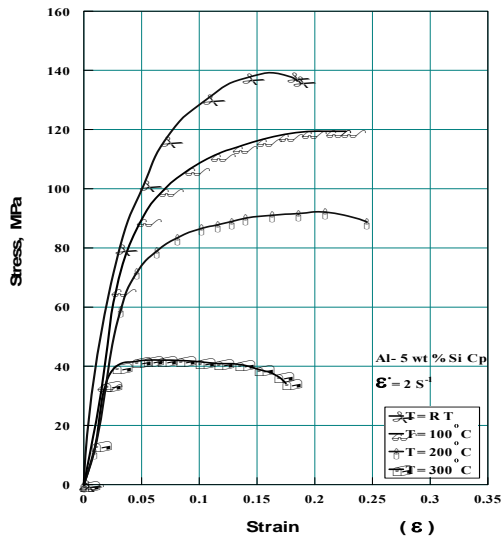


Fig. 4 Stress-Strain Curves for Al-5 wt% Si Cp at different temperature and strain rate

Fig. 5 Stress-Strain Curves for Al-10 wt% Si Cp at different temperature and strain rate

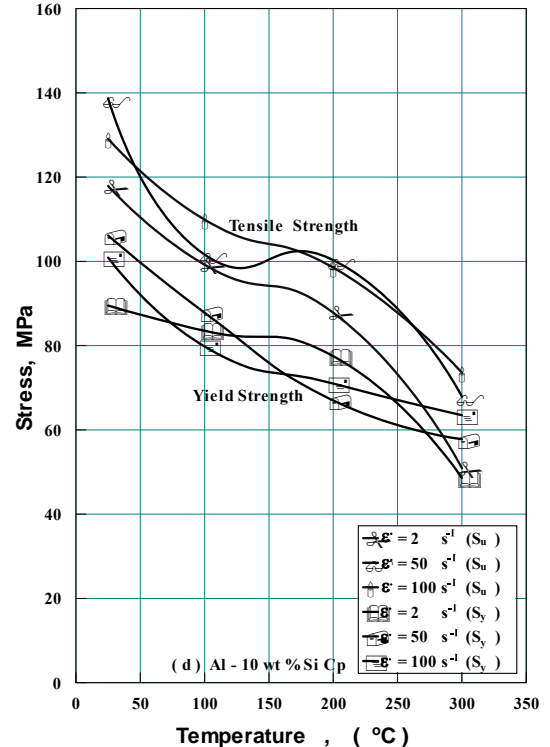
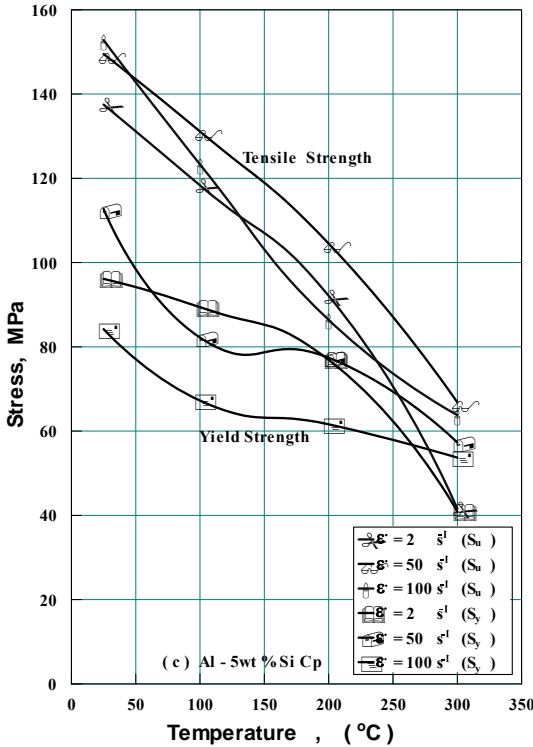
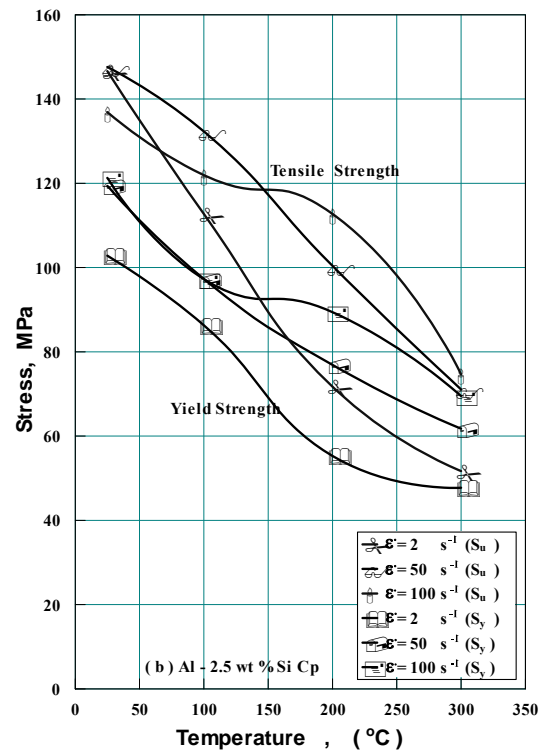
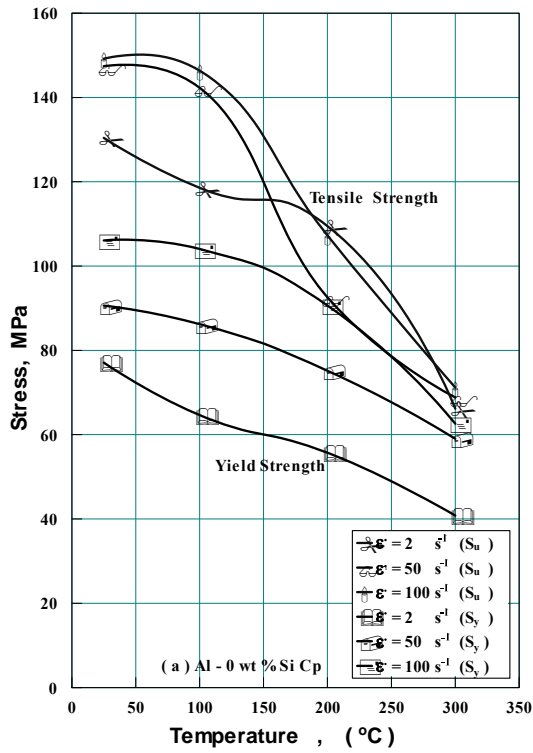


Fig. 6 Variation of Yield and Tensile Strengths with Deformation Temperatures

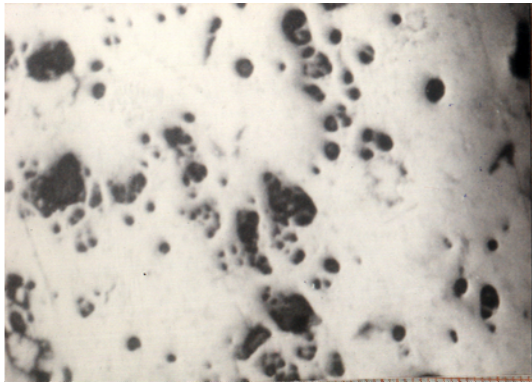


Fig. 7- a

Micrograph of Al 5wt% SiC_p (X80)

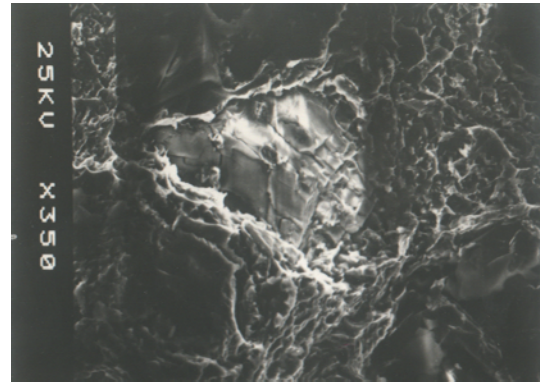


Fig. 7- b

SEM Fractograph of Al 10wt% SiC_p

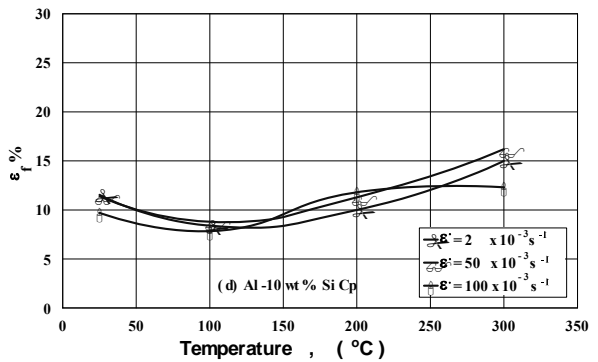
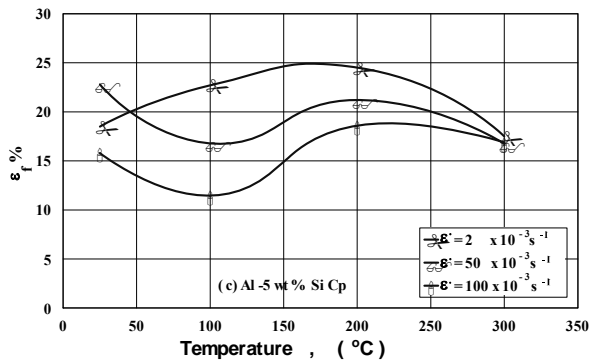
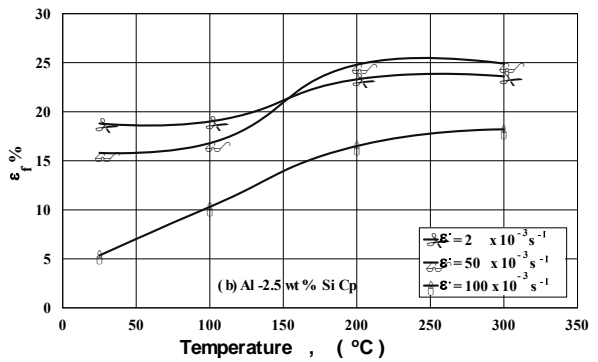
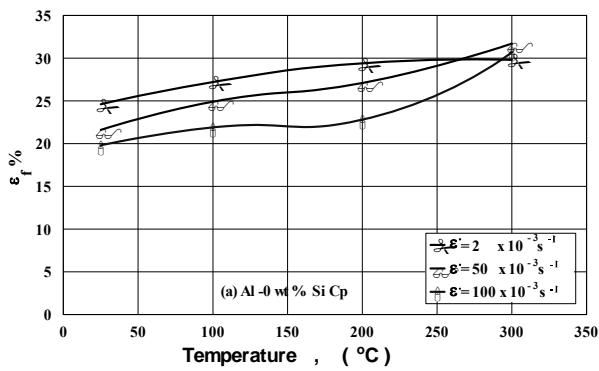


Fig. (8) Variation of Elongation to Fracture with Deformation Temperatures